Perforated materials with periodically distributed annular cavities for low frequency acoustic absorption

Thomas Dupont, Philippe Leclaire, Olga Umnova, Raymond Panneton

Perforated materials with periodically distributed annular cavities for low frequency acoustic absorption

Thomas Dupont[a)]
Département de Génie Mécanique, École de Technologie Supérieure, 1100 rue Notre-Dame Ouest, Montréal (Qc), Canada, H3C 1K3.

Philippe Leclaire[b)]
DRIVE EA1859, Univ. Bourgogne Franche Comté, ISAT, BP 31 - 49 rue Mlle Bourgeois 58027 Nevers - France.

Olga Umnova[c)]
Acoustics Research Centre, University of Salford, Salford M5 4WT, United Kingdom.

Raymond Panneton[d)]
GAUS, Département de Génie Mécanique, Université de Sherbrooke, Sherbrooke, Canada J1K 2R1.

ABSTRACT

A microstructure design of thin low-frequency resonant acoustic absorbers is proposed. A perforated material is studied, in which the main perforations are connected to a collection of periodically spaced very thin annular dead-end pores with respect to the lateral size, these absorbers are called multi-pancake materials. It has been shown in the past that the acoustical properties of perforated materials can be described by the classical theory of porous media. With the help of this model in the rigid frame approximation, it is shown that at low frequencies, the periodic array of annular dead-end pores increases the effective compressibility without modifying the effective dynamic density. Due to this effect, the first absorption peak appears at much lower frequency, compared to that of the perforated structure without dead-end pores. A transfer matrix approach is proposed to model and optimize the absorber. Prototypes have been 3D printed and tested for sound absorption and transmission loss. New materials capable of producing absorption peaks at a few hundred Hz for an overall material thickness of a few cm were designed. A good agreement between the data and the model predictions is demonstrated. New designs for broader absorption and under higher sound pressures are investigated.

[a)] email: Thomas.Dupont@etsmtl.ca
[b)] email: Philippe.Leclaire@u-bourgogne.fr
[c)] email: O.Umnova@salford.ac.uk
[d)] email: Raymond.Panneton@USherbrooke.ca

1 INTRODUCTION

The development of thin acoustic materials for low frequency absorption is an important challenge for the industry and is required in many applications, e.g. the acoustic liners for turbo fan engine, passenger compartments, or the acoustic treatments of buildings. To improve the absorption at low frequencies, systems involving Micro Perforated Plates (MPP) with extended tubes[1,2] or periodic arrays of resonators[3] were used. Boutin[4] proposed to use the homogenization method to model the acoustic of porous media with inner resonators. Based on Bradley's works[5], Leclaire et al.[6] studied a structured perforated material containing periodically spaced dead-end (DE) pores (Fig. 1). It has been observed that the presence of the periodic lattice of dead-end pores leads to the appearance of absorption peaks at low frequencies and at high frequencies (bandgap or stop bands for the sound transmission). Similar observations on other sound absorbing systems were reported by Groby et al.[7].

In reference [6], it has been proposed to model the resonant material with periodically spaced dead-end cavities by a transfer matrix approach or using low frequency asymptotic expansions. The presence of the network of DE pores has the effect, at low frequencies, of increasing the effective compressibility of the material without changing its effective dynamic density. This induces a decrease of the effective celerity of the material[7]. Due to this effect, the presence of a periodic network of pores significantly reduces the resonance frequencies of the material. This leads to the appearance of the absorption peaks at much lower frequencies without increasing the thickness of the resonant material. The model has been validated by numerical simulation and by comparing its predictions with measurements on prototype samples[6].

Based on this work, we propose a new type of microstructure design for low frequency resonant materials. In order to enhance the thermal effects at low frequencies and thus to decrease the first resonance frequency, a perforated material with a periodic lattice of very thin annular cavities (or ring, "pancake" or "mille-feuille" cavities with ratios of radii to thicknesses of 40 or more for example). The proposed microstructure is directly inspired from the design of heat exchangers. A patent application has been filed on the thin multi-pancake resonant materials[8]. The determination of the pancake cavity impedance is inspired from the work by Dickey and Selamet[9] on the acoustic behavior of a Helmholtz resonator with a "pancake" shape. A transfer matrix approach is proposed to model and optimize the absorber. Prototypes have been 3D printed and tested for sound absorption and transmission loss.

This paper is drawn from the cited article [10]. Complementary information is provided in this reference[10].

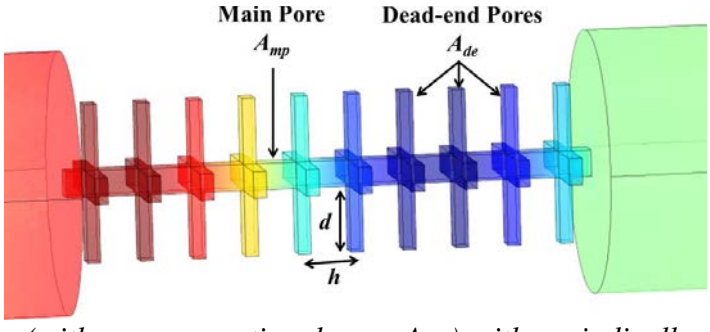

Fig. 1 – Main pore (with a cross-sectional area A_{mp}) with periodically arranged dead-end pores, n = 4 identical dead-end pores with cross-section area A_{de} and length d per period h. The dead-end pores are located at "nodes".

2 PROPOSED MICROSTRUCTURE DESIGN OF THE RESONANT MATERIAL

2.1 Low frequency approximation of the effective properties of a perforated plate with periodically spaced short dead-ends (Fig. 1)

When the wavelength λ is much greater than the spacing h and the length d of the dead-ends ($\lambda \gg h, d$), low frequency approximations for the effective density ρ_e and compressibility C_e of the air inside a perforated plate with periodically spaced short dead-ends were given as[6]:

$$\rho_e = \rho_{mp} \tag{1}$$

$$C_e = C_{mp} + C_{de}\frac{nA_{de}}{A_{mp}}\frac{d}{h} = C_{mp} + C_{de}\frac{V_{de}}{V_{mp}} \tag{2}$$

where ρ_{mp}, C_{mp} and C_{de} are respectively the density of the air in the main perforation, its compressibility and the compressibility of air in the dead-ends. n is the number of dead-ends at each node. A_{mp} and A_{de} are respectively the cross sections of the main pore and of the dead-end pores while V_{mp} and V_{de} are their respective volumes.

These equations show that a periodic array of DE pores at low frequencies does not modify the effective density of air in the main pore but it increases significantly its effective compressibility. That means that the periodic array of DE pores has a significant influence on thermal effects occurring in the thermal boundary layers near the DE pore walls. The effective compressibility (inverse of the bulk modulus) is associated with the thermal characteristic length[11].

The low frequency approximation of the effective sound speed is given by:

$$c_e = \frac{1}{Re\sqrt{\rho_e C_e}} \xrightarrow[\lambda \gg h,d]{} \frac{1}{Re\sqrt{\rho_e\left(C_{mp} + C_{de}\frac{V_{de}}{V_{mp}}\right)}} \tag{3}$$

It is clear from this equation, that periodic array of DE pores decreases sound speed in the material. If we consider a quarter-wavelength thickness L material with straight main pores only (without lateral dead-end), the first resonance frequency is given by:

$$f_{r1} = \frac{c_{mp}}{4L} \tag{4}$$

where c_{mp} is the effective sound speed in the main pore. If a periodic array of lateral DE pores is added, the effective sound speed c_e is given by equation (4), and the first resonance frequency is modified as follows:

$$f_{r1}^{*} = \frac{1}{4L}\frac{1}{Re\sqrt{\rho_e\left(C_{mp} + C_{de}\frac{V_{de}}{V_{mp}}\right)}} \tag{5}$$

Thus, periodic arrays of DE pores can reduce the first resonance frequency significantly.

2.2 Proposed resonator design

According to Eqs. (5) and (2), the resonance frequency f_{r1} can be decreased by increasing the ratio $nA_{de}d/A_{mp}h$. Central perforations should bear as many dead-end pores as possible at each node, the dead-ends pores should have large volumes and the periodic distance should be small. The different conditions found are not all compatible with one another (large DE volumes require large cross sections and long dead-ends) and with a sufficient perforation rate on the surface of the plate. Furthermore, the parameters involved in the ratio will have an effect on the compressibilities C_{mp} and C_{de} through the thermal characteristic length[10]. In a first approach, however, it is thought that the compressibilities will have less effect than this ratio; it therefore provides us with a simple design tool. The proposed microstructure is also inspired from the design of heat exchangers. The proposed design is shown on Figure 2. This "perforated pancake absorber" can be built using 3D printing technology resin (stereo-lithography process - Figure 2).

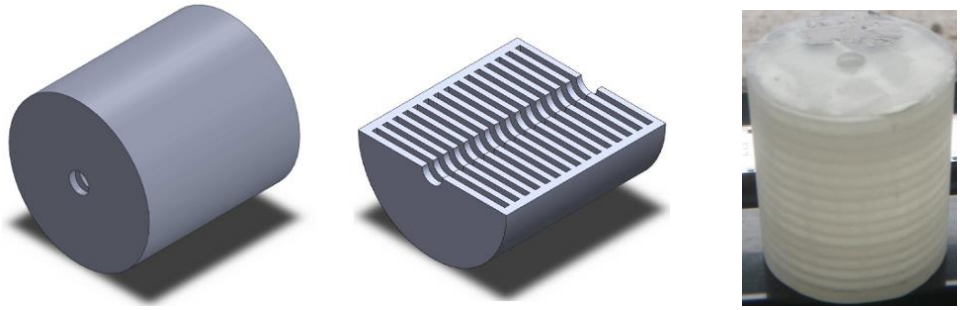

Fig. 2 – Perforated material with multiple 'pancake' cavities (sample A). The full sample is shown on the left and its longitudinal cross section is in the center. On the right a 3D printing sample which has been made using a transparent is shown*. The parameters of this sample are given in Table 1 (sample thickness sample L = 31 mm and external diameter d_{samp} = 29 mm).*

2.3 Lumped parameter model with Transfer Matrix formulation

The lump element approach is used here to account for the pancakes cavities located in parallel to the main pore. First, we consider a single cell with thickness *h* (period) composed of a main pore and a pancake cavity (see Figure 3).

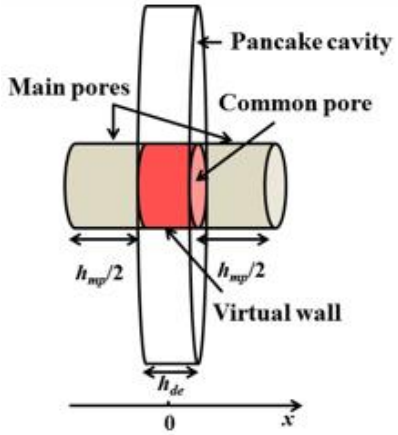

Fig. 3 – One single periodic cell composed of two halves of the main pore, a common pore and a "pancake" cavity. The common pore corresponds to the common volume between the main pore and the "pancake" cavity.

The common pore corresponds to the common volume between the main pore and the pancake cavity. Thus the single periodic cell is split up in two half main pores (with a thickness $h_{mp}/2$), a common pore and a pancake cavity (with a thickness h_{de}).

The two halves of the main pores are identified as effective fluids with parameters (wavenumber k_{mp}, characteristic impedance Z_{mp}) given by the Johnson-Champoux- Allard (JCA) model[12] for porous media. It is assumed that $Re(k_{mp}d_{mp}) \prec\prec 1$ so that the waves inside the main pores can be considered as plane waves. The transfer matrix of a main pore for a thickness $h_{mp}/2$ is given by:

$$\mathbf{T}_{mp}^{(h_{mp}/2)} = \begin{pmatrix} \cos(k_{mp}h_{mp}/2) & jZ_{mp}\sin(k_{mp}h_{mp}/2) \\ \frac{j}{Z_{mp}}\sin(k_{mp}h_{mp}/2) & \cos(k_{mp}h_{mp}/2) \end{pmatrix} \tag{6}$$

Time dependence $e^{j\omega t}$ is assumed throughout. The pancake cell is composed of a common pore and a truncated pancake cavity, the two elements are separated by a virtual wall. It is proposed to consider the common pore as an element without thermo-viscous losses. Thus, the transfer matrix of this common element for a thickness $h_{de}/2$ is given by:

$$\mathbf{T}_{com}^{(h_{de}/2)} = \begin{pmatrix} \cos(k_0 h_{de}/2) & jZ_0\sin(k_0 h_{de}/2) \\ \frac{j}{Z_0}\sin(k_0 h_{de}/2) & \cos(k_0 h_{de}/2) \end{pmatrix} \tag{7}$$

with (k_0, Z_0) are the wavenumber and characteristic impedance of air.

Then the pancake cavity is considered as a side branch (same as a DE pore) which is represented by a surface impedance $Z_{S,de}$. It is proposed to use the "pancake" cavity surface impedance expression proposed by Dickey and Selamet [9], valid for circular cross section, to model a Helmholtz resonator (one open-closed cavity) with a small cavity length-to-diameter ratio:

$$Z_{S,de} = jZ_{de}\left\{\frac{H_0^{(1)}(k_{de}r_{mp}) - \left[H_1^{(1)}(k_{de}r_{de})/H_1^{(2)}(k_{de}r_{de})\right]H_0^{(2)}(k_{de}r_{mp})}{H_1^{(1)}(k_{de}r_{mp}) - \left[H_1^{(1)}(k_{de}r_{de})/H_1^{(2)}(k_{de}r_{de})\right]H_1^{(2)}(k_{de}r_{mp})}\right\} \tag{8}$$

with $H_i^{(n)}(kr)$ the Hankel function of ith order and of nth kind of the wavenumber k and of the radial position r relatively to the center. The effective parameters (k_{de}, Z_{de}) of the air in the pancake cavity are calculated using JCA model[12]. It is assumed here that $h_{de} \prec\prec r_{de} \ll \lambda$, so the expressions for slit geometry are used (Table 2). At the center of the common pore, the admittance relation is applied. The transfer matrix of the pancake cavity (as side branch) is given by:

$$\mathbf{T}_{de} = \begin{pmatrix} 1 & 0 \\ \frac{1}{Z_{S,de}}\frac{A_{de}}{A_{mp}} & 1 \end{pmatrix} \tag{9}$$

with $A_{mp} = \pi r_{mp}^2$ the cross-section area of the main pore and $A_{de} = 2\pi r_{mp}h_{de}$ the area of the virtual wall separating the common pore and the pancake cavity.

The transfer matrix of the periodic cell with thickness $h = h_{mp} + h_{de}$ is given by:

$$\mathbf{T}_{cell} = \mathbf{T}_{mp}^{(h_{mp}/2)}\ \mathbf{T}_{com}^{(h_{de}/2)}\ \mathbf{T}_{de}\ \mathbf{T}_{com}^{(h_{de}/2)}\ \mathbf{T}_{mp}^{(h_{mp}/2)} \tag{10}$$

Our material is constituted of a series of *N* pancake cavities. The transfer matrix is given by:

$$\mathbf{T}_{samp} = \mathbf{T}_{end\,2}\left(\mathbf{T}_{cell}\right)^{N}\mathbf{T}_{end\,2} \tag{11}$$

with $\mathbf{T}_{end1}$ and $\mathbf{T}_{end2}$ the transfer matrix which includes the pore end effect and the contraction effect[10]. The normal sound absorption coefficient of the absorber (for a rigidly backed sample) and its normal sound transmission loss (for the configuration which the sample is coupled to two semi-infinite regions) are then calculated using $t_{samp,ij}$ of eq. 11 :

$$\alpha_N = 1 - \left|\frac{t_{samp,11} - t_{samp,21}Z_0}{t_{samp,11} + t_{samp,21}Z_0}\right|^2, \quad TL = -20\log_{10}\left|\frac{2}{t_{samp,11} + t_{samp,22} + t_{samp,12}/Z_0 + t_{samp,21}Z_0}\right| \tag{13}$$

3 NUMERICAL APPROACH AND EXPERIMENTAL DETAILS

It is proposed to compare the semi analytical results with those obtained numerically in a virtual tube. The virtual measurements are obtained with a three dimensional acoustical FEM simulations using COMSOL Multiphysics software. A three-microphone method[13] is used to get the virtual measurements. The elements of the absorbers were modeled as those filled with effective fluids given by JCA model as outlined in Table 2. The details of the numerical approach are given in reference [10].

For the experimental measurements, an acoustic tube with cross section diameter with $d_{tube} = 29\ mm$ is used. The frequency range is between 100 Hz to 6400 Hz. The four-microphone method[14,15] is used. Several samples have been tested. The results have been averaged over several measurements. Then the results are presented with the mean value $\bar{x}$ and the expanded uncertainty with a coverage factor $h = 1$: $x = \bar{x} \pm h\sigma$, with σ the standard deviation.

The absorption coefficient results are presented for the configuration in which the sample is backed by a rigid wall. The transmission loss results are presented for configuration in which the sample is coupled to two semi-infinite regions. The complete experimental details are given in reference [10].

5 ANALYTICAL, NUMERICAL AND EXPERIMENTAL RESULTS

5.1 Material parameters for the models

One prototype (sample A) is presented in this article, a second prototype (the sample B) has been presented in reference [10]. Both prototypes are designed to be tested in the impedance tube. An external diameters for sample A is proposed; $d_{samp} = 29\ mm$, corresponding to the acoustic tubes cross-section diameter. The samples have a thickness of $L = 31\ mm$, Table 1 summarizes the sample parameters. The effective fluid parameters of the main pore are given in Table 2.

Table 1 - Parameters of the multi-pancakes samples.

	d_{samp} (mm)	d_{mp} (mm)	d_{de} (mm)	h_{mp} (mm)	h_{de} (mm)	N	L (mm)
Sample A	29	4	26	1	1	15	31
Sample B[10]	44.4	4	40	1	1	15	31

Table 2 - Johnson-Champoux-Allard (JCA) parameters of the main pore and pancake cavity, with η the dynamic viscosity of air.

	Viscous length Λ (mm)	*Thermal length* Λ' *(μm)*	*Tortuosity* α_∞	*Static air flow resistivity* σ *(Pa·s/m²)*	*Open porosity* ϕ *(%)*
Main pore (circular pore)	r_{mp}	r_{mp}	1	$8\eta/(r_{mp}^2\phi)$	1
"Pancake" cavity (slit)	h_{de}	h_{de}	1	$12\eta/(h_{de}^2\phi)$	1

5.2 Results

The measured and simulated normal incidence sound absorption coefficient of the rigidly backed sample A and the normal sound transmission loss of sample A (in transmission configuration) are presented in Figure 4. The first absorption peak is high (close to *100%*) and its frequency is around *550 Hz*. This frequency is equal to the first resonance frequency of a perforated material without pancake cavities (quarter-wavelength tube resonance) with a thickness $L^*= 4.8$ $L = 148$ *mm*. Thus, for these samples, adding periodic array of pancake cavities allows reduction in thickness by a factor of *4.8*. The first resonance of the perforated sample without pancake cavities with same thickness $L= 31$ *mm* is $f_{res^*} = 2578$ *Hz*. The agreement between the models and the experiments is very good for the first absorption peak (see Table 3 for the values of the frequency and the amplitude of the first and the second sound absorption peaks).

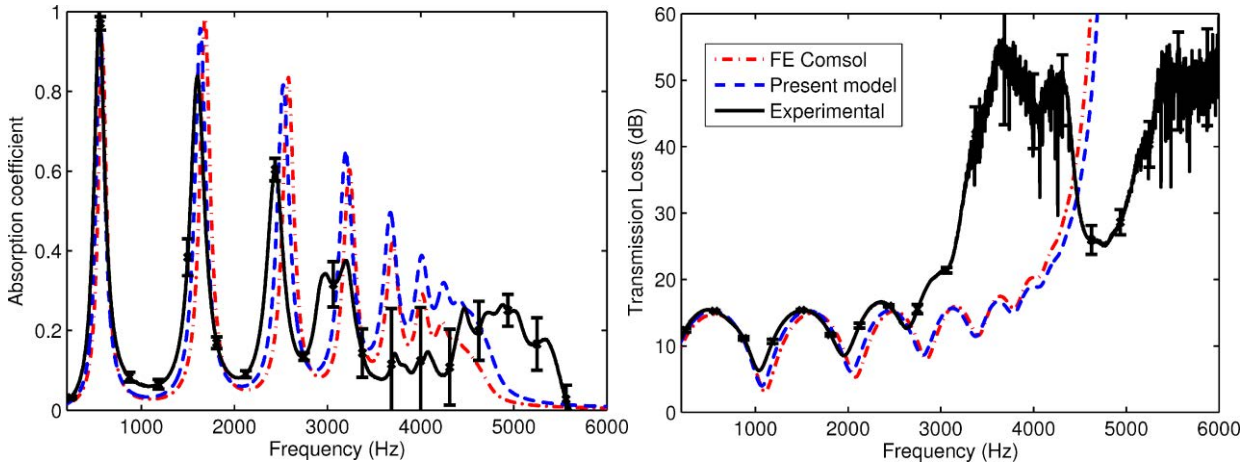

Fig. 4 – Normal sound absorption coefficient (abs. configuration: sample backed by a rigid wall) and normal sound transmission loss (transmission configuration) of the sample A (perforated multi-pancake cavity with 29 mm external diameter). The three curves correspond to: results measured in the impedance tube (---), results simulated by Finite Element approach with rigid frame assumption (-.-.-), results simulated by TMM approach (- - -).

For the second and the third absorption peaks, the models (TMM and numerical for rigid frame) predict a slightly smaller frequency shift than observed and overestimate the amplitudes. Above 2500 Hz, both models fail to correctly predict the acoustic behavior of the tested sample. The discrepancies are thought to be caused by several effects including the resonance effect due to elasticity of the material and stopband effects occurring in certain frequency bands. The agreement between the present TMM model and the numerical (FE) model is good in the studied frequency range. However, a noticeable difference is found on the absorption peak frequencies and amplitudes (see Table 3), especially above 3000 Hz. This discrepancy could be explained by the fact that plane wave assumption has been considered in the TMM model.

Table 3 - Mean frequency values and mean amplitudes of the first and the second absorption peaks for sample A. The results are given for the experimental approach, the present model and the two FEM models (with rigid frame assumption and with elastic frame assumption).

	Frequency (Hz) 1st peak	Amplitude (%) 1st peak	Frequency (Hz) 2nd peak	Amplitude (%) 2nd peak
Experimental	550	99.7	1603	83.8
Present model (TMM)	560	97.8	1634	95.8
FEM model (rigid frame)	580	91.9	1680	98.4
FEM model (elastic frame)	580	88.7	1680	98.8

Moreover, due to periodicity of the pore structure, it can be observed that the models predict a stopband above 4700 Hz (the stopband corresponds to absorption coefficient dropping to zero and the transmission loss raising to high values). However, the analysis of the transmission loss shows that there are two stopband effects; one is between 3500 Hz and 4200 Hz and the second is above 5500 Hz. To attempt to explain the two observed experimental stop bands, a numerical model with elastic frame assumption was used (COMSOL Multiphysics software with vibro-acoustic option). Mechanical parameters of the Acrylonitrile Butadiene Styrene (ABS); with the density $\rho_s = 1040\ kg/m^3$, the Young's modulus $E = 2275\times10^6$ Pa, and the Poisson's ratio $v = 0.35$ were used in the model. The results are shown on Figure 5. Accounting for frame elasticity leads to appearance of low absorption coefficient in the frequency range between 3.5 kHz and 4.2 kHz. It would appear that there would therefore be two bandgap effects; the first one corresponding to a vibrational bandgap effect (vibrational resonance of the membrane in periodic array arrangement[16]) and the second one corresponding to an acoustic bandgap effect (acoustic resonance of the pancake cavities in periodic array arrangement). Indeed the first natural frequency of flexural vibrations of a circular ABS plate (similar to the wall between two pancake cavities) is found[17] in vacuo condition between 2149 Hz (with "simply supported" boundary conditions) and 4383 Hz (with "clamped" boundary conditions). The real boundary conditions for the wall of pancake cavities are between "simply supported" and "clamped". Thus the first natural frequency of flexural vibrations is included in the first bandgap frequency bandwidth. Moreover the first acoustic resonance of the pancake cavity is 5239 Hz; this frequency is included in the second bandgap frequency bandwidth. It can be noticed that similar two bandgap effects have been observed for an acoustic metamaterial composed of a periodically arranged Helmholtz resonators and membranes[18].

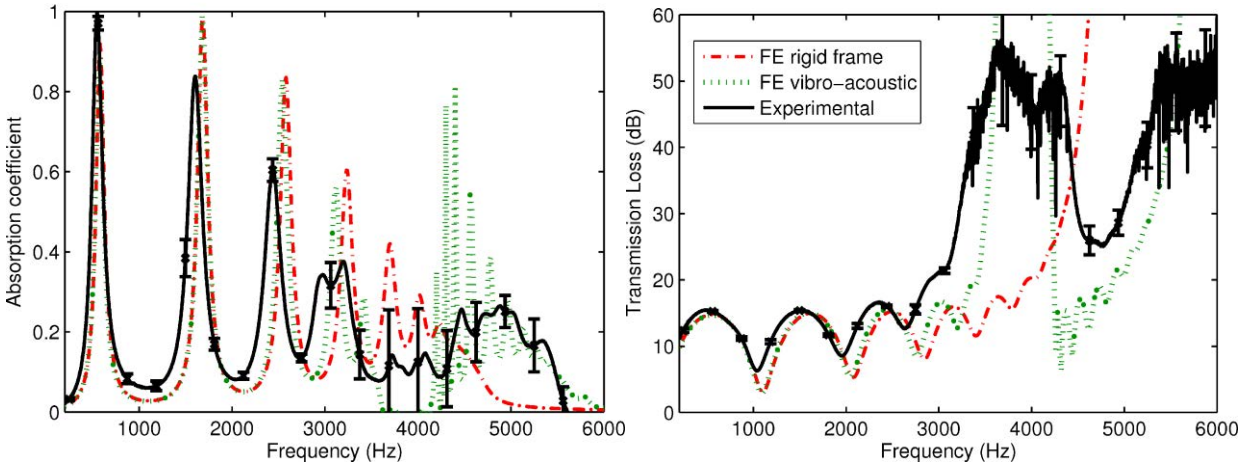

Fig. 5 – Normal sound absorption coefficient (abs. configuration: sample backed by a rigid wall) and normal sound transmission loss (trans. configuration) of the sample A (perforated multi-pancake cavity with 29 mm external diameter). The curves correspond to: results measured in the impedance tube (---), results simulated by Finite Element approach with rigid frame assumption (-.-.-), results simulated by Finite Element vibro-acoustic approach (with elastic frame) (. . .).

Note that in reference [10] the prototype B was presented, the diameter was increased (with an external diameter d_{samp} = *44.4 mm,* the pancake cavity diameter is d_{de} = *40 mm*) in order to increase the pancake cavity volume and therefore decrease the first absorption peak (see Eq. 5). The first absorption peak is observed around 392 Hz, which means that adding a periodic array of pancake cavities allows the reduction in thickness by a factor of 6.6 compared to simply perforated sample (quarter-wavelength tube), moreover the amplitude of the absorption peak is preserved.

6 CONCLUSIONS

Based on the low frequency approximation of effective parameters of a structured perforated material containing periodically spaced dead-end pores, a microstructure design for low frequency sound absorber materials was proposed in this work. It corresponds to a perforated material with a periodic lattice of internal "pancake" cavities. Sound absorber prototypes have been made and tested in the impedance tube. The periodic lattice of "pancake" cavities allows decreasing significantly the frequencies of the absorption peaks without increasing the thickness of the sample. Moreover two stopband effects have been observed for these materials at higher frequencies: the first stopband is due to the acoustic resonance of the periodic pancake cavities and the second to the frame resonance of the sample.

Future works are concerned with the optimization of the microstructure to improve the low frequency absorption properties. Studies are in progress in order to enlarge the absorber frequency bandwidth (especially at mid and high frequencies) and to optimize the frequency value of the first absorption peak (lower as possible).

7 REFERENCES

1. D. Li, D. Chang, B. Liu, "Enhancing the low frequency sound absorption of a perforated panel by parallel-arranged extended tubes", *Applied Acoustics,* **102**, 126–132, (2016).

2. F. Simon, “Long Elastic Open Neck Acoustic Resonator for low frequency absorption”, *J. Sound. Vib.*, **421**, 1-16, (2018).
3. C. Lagarrigue, J.-P. Groby, V. Tournat, and O. Umnova, “Absorption of sound by porous layers with embedded periodic array of resonant inclusions”, *J. Acoust. Soc. Am.*, **134**, 4670-4680, (2013).
4. C. Boutin, “Acoustics of porous media with inner resonators”, *J. Acoust. Soc. Am.*, **134**, 4717, (2013).
5. C. E. Bradley, “Time harmonic Bloch wave propagation in periodic waveguides. Part I. Theory”, *J. Acoust. Soc. Am.*, **96**, 1844-1853, (1994).
6. P. Leclaire, O. Umnova, T. Dupont, and R. Panneton, “Acoustical properties of air-saturated porous material with periodically distributed dead-end pores”, *J. Acoust. Soc. Am.*, **137**(4): 1772-1782, (2015).
7. J.-P. Groby, W. Huang, A. Lardeau, and Y. Aurégan, “The use of slow waves to design simple sound absorbing materials”, *J. Appl. Phys.*, **117**, 124903 (2015).
8. P. Leclaire, T. Dupont and S. Aivazzadeh, inventors, Universite de Bourgogne, assignee. “Résonateur acoustique de faible épaisseur de type mille-feuille perforé pour l'absorption ou le rayonnement acoustique très basses fréquences (Low thickness perforated mille-feuille acoustic resonator for absorbing or radiating very low acoustic frequencies)”, *International patent* WO 2017134125 A1. 2017 Aug 10.
9. N. S. Dickey and A. Selamet, “Helmholtz resonators: One-dimensional limit for small cavity length-to-diameter ratios”, *J. Sound Vib.*, **195**(3), 512-517 (1996).
10. T. Dupont, P. Leclaire, R. Panneton and O. Umnova. A microstructure material design for low frequency sound absorption. Applied Acoustics, 136: 86-93 (2018)
11. Y. Champoux and J. F. Allard, “Dynamic tortuosity and bulk modulus in air-saturated porous media”, J. Appl. Phys., **70**, 1975-9, (1991).
12. J. F. Allard and N. Atalla, *Propagation of Sound in Porous Media: Modelling Sound Absorbing Materials* 2nd ed. John Wiley and Sons, New York, (2009).
13. Y. Salissou, O. Doutres, R. Panneton, “Complement to standard method for measuring normal incidence with three microphones” *J. Acoust. Soc. Am.*, **131**: EL216 (2012).
14. ASTM E 2611-09, “Standard test method for measurement of normal incidence sound transmission of acoustical materials based on the transfer matrix method”.
15. ISO 10534-2, “Acoustics—Determination of sound absorption coefficient and impedance in impedance tubes. Part 2: Transfer-function method”, International Organization for Standardization, Geneva, Switzerland 1998.
16. S. H. Lee, C. M. Park, Y. M. Seo, Z. G. Wang, and C. K. Kim, “Acoustic metamaterial with negative density”, Phys. Lett. A, **373**, 4464 (2009).
17. A. Zagrai and D. Donskoy, “A soft table for the natural frequencies and modal parameters of uniform circular plates with elastic edge support” *J. Sound Vib.*, **287**, 343–351 (2005).
18. Y. M. Seo, J. J. Park, S. H. Lee, C. M. Park, C. K. Kim, “Acoustic metamaterial exhibiting four different sign combinations of density and modulus”, J. Appl. Phys., **111**, 023504 (2012).